Effects of gene replacement therapy with resamirigene bilparvovec (AT132) on skeletal muscle pathology in X-linked myotubular myopathy: results from a substudy of the ASPIRO open-label clinical trial

Michael W. Lawlor,[a,b,*] Benedikt Schoser,[c] Marta Margeta,[d] Caroline A. Sewry,[e,f] Karra A. Jones,[g] Perry B. Shieh,[h] Nancy L. Kuntz,[i] Barbara K. Smith,[j] James J. Dowling,[k] Wolfgang Müller-Felber,[l] Carsten G. Bönnemann,[m] Andreea M. Seferian,[n] Astrid Blaschek,[l] Sarah Neuhaus,[m] A. Reghan Foley,[m] Dimah N. Saade,[m] Etsuko Tsuchiya,[k] Ummulwara R. Qasim,[h] Margaret Beatka,[a,b] Mariah J. Prom,[a,b] Emily Ott,[a,b] Susan Danielson,[a] Paul Krakau,[a,b] Suresh N. Kumar,[a] Hui Meng,[a,b] Mark Vanden Avond,[a] Clive Wells,[a] Heather Gordish-Dressman,[o] Alan H. Beggs,[p] Sarah Christensen,[q] Edward Conner,[q] Emma S. James,[q] Jun Lee,[q] Chanchal Sadhu,[q] Weston Miller,[q] Bryan Sepulveda,[q] Fatbardha Varfaj,[q] Suyash Prasad,[q] and Salvador Rico[q]

[a]Medical College of Wisconsin, Department of Pathology and Laboratory Medicine, Milwaukee, WI, 53226, USA
[b]Diverge Translational Science Laboratory, Milwaukee, WI, 53204, USA
[c]Friedrich-Baur-Institute, Department of Neurology, Ludwig Maximilian University of Munich, 80336, Germany
[d]Department of Pathology, University of California San Francisco, San Francisco, CA, 94143, USA
[e]Wolfson Centre of Inherited Neuromuscular Disorders, RJAH Orthopaedic Hospital, Oswestry, SY10 7AG, UK
[f]Dubowitz Neuromuscular Centre, UCL Institute of Child Health and Great Ormond Street Hospital for Children, 30 Guilford Street, London, WC1N 1EH, UK
[g]Department of Pathology, Duke University School of Medicine, Durham, NC, 27710, USA
[h]Department of Neurology, University of California Los Angeles School of Medicine, Los Angeles, CA, 90095, USA
[i]Ann & Robert H Lurie Children's Hospital of Chicago, Chicago, IL, 60611, USA
[j]Department of Physical Therapy, University of Florida, Gainesville, FL, 32610-0154, USA
[k]Hospital for Sick Children, Toronto, ON, M5G 1X8, Canada
[l]Dr. von Hauner Children's Hospital, Klinikum der Universität München, 80337, Munich, Germany
[m]Neuromuscular and Neurogenetic Disorders of Childhood Section, NINDS, NIH, Bethesda, MD, 20892-1477, USA
[n]I-Motion, Hôpital Armand Trousseau, 75571, Paris, France
[o]Children's National Hospital and George Washington University School of Medicine and Health Sciences Department of Pediatrics, Washington, DC, 20037, USA
[p]Division of Genetics and Genomics, The Manton Center for Orphan Disease Research, Boston Children's Hospital, Harvard Medical School, Boston, MA, 02115, USA
[q]Formerly of Astellas Gene Therapies (formerly Audentes Therapeutics, Inc.), San Francisco, CA, 94108, USA

eBioMedicine
2023;99: 104894
Published Online xxx
https://doi.org/10.1016/j.ebiom.2023.104894

Summary

Background X-linked myotubular myopathy (XLMTM) is a rare, life-threatening congenital muscle disease caused by mutations in the *MTM1* gene that result in profound muscle weakness, significant respiratory insufficiency, and high infant mortality. There is no approved disease-modifying therapy for XLMTM. Resamirigene bilparvovec (AT132; rAAV8-Des-hMTM1) is an investigational adeno-associated virus (AAV8)-mediated gene replacement therapy designed to deliver *MTM1* to skeletal muscle cells and achieve long-term correction of XLMTM-related muscle pathology. The clinical trial ASPIRO (NCT03199469) investigating resamirigene bilparvovec in XLMTM is currently paused while the risk:benefit balance associated with this gene therapy is further investigated.

Methods Muscle biopsies were taken before treatment and 24 and 48 weeks after treatment from ten boys with XLMTM in a clinical trial of resamirigene bilparvovec (ASPIRO; NCT03199469). Comprehensive histopathological analysis was performed.

Findings Baseline biopsies uniformly showed findings characteristic of XLMTM, including small myofibres, increased internal or central nucleation, and central aggregates of organelles. Biopsies taken at 24 weeks post-treatment showed marked improvement of organelle localisation, without apparent increases in myofibre size in most participants. Biopsies taken at 48 weeks, however, did show statistically significant increases in myofibre

*Corresponding author. Diverge Translational Science Laboratory, 247 Freshwater Way, Suite 600, Milwaukee, WI, 53204, USA.
E-mail address: mlawlor@divergetsl.com (M.W. Lawlor).

size in all nine biopsies evaluated at this timepoint. Histopathological endpoints that did not demonstrate statistically significant changes with treatment included the degree of internal/central nucleation, numbers of triad structures, fibre type distributions, and numbers of satellite cells. Limited (predominantly mild) treatment-associated inflammatory changes were seen in biopsy specimens from five participants.

Interpretation Muscle biopsies from individuals with XLMTM treated with resamirigene bilparvovec display statistically significant improvement in organelle localisation and myofibre size during a period of substantial improvements in muscle strength and respiratory function. This study identifies valuable histological endpoints for tracking treatment-related gains with resamirigene bilparvovec, as well as endpoints that did not show strong correlation with clinical improvement in this human study.

Funding Astellas Gene Therapies (formerly Audentes Therapeutics, Inc.).

Keywords: X-linked myotubular myopathy; Centronuclear myopathy; Gene replacement therapy; Adeno-associated viral vector; Pathology; Human

Research in context

Evidence before this study

The skeletal muscle pathology observed in X-linked myotubular myopathy (XLMTM) is highly characteristic and includes marked myofibre smallness, mislocalisation of organelles, and an increased proportion of fibres with centrally or internally placed nuclei, based on evidence from skeletal muscle biopsies from patients with XLMTM. The effect of disease-modifying treatment with gene therapy on the muscle pathology of individuals with XLMTM has not previously been described. We searched PubMed for publications describing gene therapy for X-linked myotubular myopathy from January 1, 2000 to August 3, 2017 (the start date of the ASPIRO study), using the search terms ("X-linked myotubular myopathy" OR "XLMTM" OR "X-linked centronuclear myopathy" OR "myopathies, structural, congenital/drug therapy [MeSH terms]") AND "gene therapy" and found no relevant articles. A separate literature search combining XLMTM terms with "myopathies, structural, congenital/pathology [MeSH terms]", "muscle, skeletal/pathology [MeSH terms]" or "muscle, skeletal/drug effects [MeSH terms]" identified studies where the histopathologic effects of *MTM1* gene transfer have been explored in animal models of XLMTM. Indeed, murine and canine models of XLMTM display similar pathological findings to those observed in human XLMTM disease, and AAV-MTM1 gene therapy in these models can reverse the pathology within 8 weeks of treatment. Following these successful preclinical studies, increases in muscle strength and motor function have been demonstrated in boys with XLMTM participating in the ongoing ASPIRO clinical trial of gene replacement therapy with rAAV8-Des-hMTM1 (resamirigene bilparvovec), and this study provides a detailed investigation of muscle biopsy pathology before and after vector administration from the first ten participants dosed in the trial.

Added value of this study

The ASPIRO study is the first clinical trial of gene replacement therapy or any disease-modifying therapy for XLMTM. This pathology substudy focuses on evaluation of baseline and post-treatment muscle biopsies using a broad array of pathological endpoints that have been reported in humans with XLMTM or animal models of XLMTM. The report provides details on the execution of muscle biopsy studies and presents results demonstrating several key improvements in pathology that correlate with functional improvement. Conversely, there are also pathological findings that do not correlate with functional improvement, and the learnings here provide important context for the pathophysiology of muscle weakness in XLMTM and for relevant endpoints in future human studies of this disease.

Implications of all the available evidence

Our findings demonstrate that pathological recovery in boys with XLMTM dosed with resamirigene bilparvovec in the ASPIRO study occurs less completely and much more slowly in comparison to post-treatment changes in XLMTM animal models, which is an important consideration in clinical trial design and planning. The practices developed in this study in relation to muscle biopsy collection, processing, and analysis provide a roadmap for successful clinical trial operations in studies that require muscle biopsies. This study defines a subset of pathological endpoints that correlate to functional improvements and a subset that do not display such a correlation, thereby identifying the pathological endpoints most likely to be useful for future studies in this disease.

Introduction

X-linked myotubular myopathy (XLMTM) is a rare, life-threatening congenital muscle disease caused by pathogenic mutations in the *MTM1* gene, leading to an absence or insufficiency of functional myotubularin protein. Without functional myotubularin, individuals with XLMTM experience profound muscle weakness, significant respiratory insufficiency, dependence on mechanical ventilation, and high mortality rate.[1–5] Up to half of infants with XLMTM may die before 18 months of age, with mortality typically attributed to respiratory failure or related complications.[1,3] Skeletal muscle biopsies from patients with XLMTM display myofibre smallness, mislocalisation of organelles, and increased numbers of myofibres with centrally or internally placed nuclei on light microscopy, and decreased or abnormal-appearing triads on electron microscopy.[6]

There are currently no approved disease-modifying therapies for XLMTM. Resamirigene bilparvovec (AT132; rAAV8-Des-hMTM1) is an investigational adeno-associated virus (AAV)-mediated gene replacement therapy administered as a one-time intravenous infusion. It is designed to deliver a functional human *MTM1* gene to skeletal muscle cells under the control of the muscle-specific desmin promoter and achieve long-term correction of XLMTM-related muscle pathology. Increased myotubularin expression and significant phenotypic improvement have been demonstrated in established mouse and canine models of XLMTM following a single administration of AAV vectors expressing *MTM1*.[7–10] Pronounced correction of pathological findings were observed at the light microscopic level, which were maintained throughout 6 months of follow-up in mice,[8] and for at least 4 years in dogs.[9]

The ASPIRO clinical trial (NCT03199469) is evaluating the safety and efficacy of resamirigene bilparvovec in boys with XLMTM. Results for the full study cohort, in which 17 participants received 3.5×10^{14} vector genomes/kilogram (vg/kg), 7 received 1.3×10^{14} vg/kg, and 14 served as untreated controls, are published elsewhere.[11] In summary, there were significant and clinically important improvements in ventilator dependence and motor function at week 24 after dosing in both dose groups, with some achieving ventilator independence and/or attaining the ability to walk independently. The most common adverse events were pyrexia (58%), increases in creatine phosphokinase (50%), and upper respiratory tract infections (~40%). Serious adverse events included infections (54%); and hepatobiliary (29%), gastrointestinal (21%), respiratory/thoracic/mediastinal (21%), and cardiac (17%) disorders.[11] Four boys who received resamirigene bilparvovec in the ASPIRO study (three at 3.5×10^{14} vg/kg and one at 1.3×10^{14} vg/kg) have died following severe cholestatic liver dysfunction.[11,12] Here we present an in-depth histopathological assessment of skeletal muscle biopsies collected from the first ten participants dosed in the trial, with focused attention to biopsy findings in relation to key endpoints of safety and efficacy. The four boys who died are not among the participants included in this pathology substudy; those events do not affect the muscle biopsy pathology presented here. At present, the ASPIRO trial is on clinical hold, while the risk:benefit balance associated with resamirigene bilparvovec for XLMTM is further investigated.

Methods

Clinical trial design

The clinical trial design and primary results of the ASPIRO study have been described in detail elsewhere.[11] ASPIRO was designed as an open-label, multinational, randomised trial of two dose levels of resamirigene bilparvovec: 1.3×10^{14} vg/kg of body weight (lower dose) and 3.5×10^{14} vg/kg (higher dose). During the trial, a series of important unexpected events resulted in major changes to the study protocol and the conduct of the trial; those changes are described in detail in the primary publication.[11] Briefly, the higher dose was originally chosen for further examination in Part 2 of the study. However, it was no longer considered after the deaths of three clinical trial participants who received the higher dose, resulting in the first clinical hold. After the hold was lifted, another boy's death associated with the administration of the lower dose led to a second clinical hold, which remains in effect at the time of this publication. As of 28 February 2022, 24 participants received resamirigene bilparvovec via a single-dose intravenous infusion (seven at the lower dose and 17 at the higher dose). Study participants included in the pathology substudy were enrolled at seven clinical study sites located in North America and Europe (Supplementary Appendix). Eligible participants were males aged 4 years and younger at dosing with a genetically confirmed diagnosis of XLMTM and met inclusion criteria defined in Supplementary Table S1. Individuals who previously participated in the prospective INCEPTUS run-in study (NCT02704273) could be older than 4 years at dosing.

To mitigate potential T cell-mediated hepatic inflammation observed in previous AAV gene therapy trials,[13,14] participants received prednisolone 1 mg/kg daily beginning one day prior to resamirigene bilparvovec infusion. The planned immunosuppressive regimen of 4 weeks followed by a 4-week taper was extended to 8 weeks plus 8-week taper after two participants developed transaminase and troponin I increases, respectively, at 7 weeks post infusion, as previously described.[11]

Randomisation and masking

Details of the original randomisation procedures of study participants to treatment or delayed control within each dose cohort are reported in detail elsewhere.[11] There were no masking procedures in this open-label

study. Randomisation was not employed for the pathology substudy.

Pathology substudy

Three discrete treatment groups were defined for histopathological analysis based on 1) resamirigene bilparvovec dose level and 2) immunosuppressive regimen. Treatment Group 1 (Participants 17, 08, and 05) received lower-dose resamirigene bilparvovec with short-duration immunosuppression (prednisolone for 4 weeks prior to tapering); Treatment Group 2 (Participants 20, 21, and 19) received lower-dose resamirigene bilparvovec with long-duration immunosuppression (prednisolone for 8 weeks prior to tapering); and Treatment Group 3 (Participants 25, 01, 23, and 02) received higher-dose resamirigene bilparvovec with long-duration immunosuppression.

Muscle biopsy acquisition and handling

Each participant had a muscle biopsy taken from the left lateral gastrocnemius (baseline), right lateral gastrocnemius (24 weeks post-treatment), and either vastus lateralis (48 weeks post-treatment). Selection of these muscles was based on 1) knowledge that gastrocnemius muscle mass in XLMTM is insufficient to allow repeated biopsy of the same muscle, and 2) autopsy evidence from individuals with XLMTM that pathology and fibre size from the gastrocnemius and vastus lateralis muscles are similar (Supplementary Figure S1).

All biopsies were open muscle biopsies obtained from muscles that had not been previously biopsied and with sampling at the belly of the muscle in areas with minimal fibrous or fatty change. Intraoperative imaging was not performed, but in some cases preoperative MRI or ultrasound imaging was used to identify high-quality areas of muscle for sampling. Tissues were processed immediately after muscle collection for evaluation of tissue endpoints (Supplementary Figure S1). Muscle tissue was frozen in isopentane cooled in liquid nitrogen according to standard procedures.[15] Samples were shipped to Cerba Research, a central laboratory logistics organisation; portions for pathological assessment (isopentane-frozen or glutaraldehyde-fixed muscle tissue portions for electron microscopy) were shipped to the central pathology laboratory at the Medical College of Wisconsin (Supplementary Appendix). All outcome data were entered into the electronic case report form using a validated web-based application. All materials generated by the study sites in support of the pathology report, including records, specimens, raw data, and any signed pathology reports were maintained in the Muscle Research Pathology archives located at the Medical College of Wisconsin and subsequently transferred to Diverge Translational Science Laboratory.

Tissue staining

Upon receipt of muscle tissue for histology assessment, internal blinding identifiers were assigned, and a single haematoxylin and eosin (H&E)-stained slide was prepared and assessed to evaluate tissue adequacy and freezing quality. Thawing/refreezing of some samples using previously described methods[15] was necessary on some biopsies due to the presence of significant freezing artifacts (including the baseline biopsy for Participant 20 and the week-48 biopsies for Participants 05, 08, 20, and 23). For pathological assessment, all samples were cut at 8-µm thickness and stained with H&E, NADH-TR, PAS, immunohistochemically stained with CD3, CD4, CD8, CD20, CD68, and C5b-9. Dual immunofluorescence staining for dystrophin and various subtypes of myosin (embryonic, foetal, slow, fast) was performed for the automated assessment of myofibre size and type. Whole slide scans were obtained at the Children's Hospital of Wisconsin Research Institute's (CRI) Imaging Core Facility using a Nanozoomer HT2 scanner with NDPI software for brightfield indications and an Olympus VS120 scanner with OlyVia software for fluorescence. Later in the study (following unblinding), additional immunohistochemical staining for p62, LC3, LAMP2, major histocompatibility complex 1, NCAM, C4d, Pax7, and FoxP3 was performed to address additional biological questions. The antibodies used for all immunostaining analysis are listed in Supplementary Table S2.

Measurement of myofibre size and type

As type 1 fibre predominance and severe myofibre smallness are features of XLMTM pathology, myofibre size and type were evaluated as potential efficacy endpoints. Myofibre size and type was measured in an automated fashion using a Visiopharm® image analysis software (App 10164) available in the CRI Imaging Core Facility, using algorithms developed specifically for this purpose in muscle tissue. The quality of the automated analysis was previously evaluated by comparison to manual measurements of the same fields in our laboratory. MinFeret diameter was used as a primary measure of myofibre size since this parameter represents a size property that is minimally dependent on fibre orientation and therefore is amenable to automated, non-biased measurement. The image used for fibre size quantification was a slide immunostained for dystrophin (to identify myofibre edges) and slow isoform of myosin heavy chain (MHCslow), and all measurements were made in Visiopharm with respect to whether the fibre was positive or negative for the MHCslow. Additional immunofluorescence slides stained for dystrophin and either the fast, foetal, or embryonic isoforms of myosin (MHCfast, MHCneo, and MHCdev, respectively) were evaluated and described during the pathological analysis of the samples, but these did not undergo formal quantification. Following data acquisition of fibre size on MHCslow slide scans, fibre size data from positive and negative fibres were pooled for a given sample. Each sample was visually assessed to

identify and measure the smallest and largest fibres manually, and this allowed a sample-specific threshold for the maximum and minimum fibre measurement for subsequent data analysis. All measurements between these sample-specific values were included in the construction of frequency histograms and cumulative probability plots in the further assessment of fibre size.

Quantification of internally or centrally nucleated fibres

Slide scans of H&E-stained sections were used by the CRI Imaging Core Facility for the automated detection of fibres containing nuclei that were not adjacent to the sarcolemma. A specialised algorithm within the Visiopharm software package was developed for this purpose (Visiopharm, Hoersholm, Denmark) and its performance was established in comparison to a subset of manually quantified samples. Following analysis, values and screen masks were quality control checked by the Lead Pathologist to ensure that the assignment of internally nucleated fibres was appropriate.

Quantification of organelle mislocalisation

Mislocalisation of organelles (usually corresponding to central aggregates of organelles with a subsarcolemmal halo, but more rarely observed as ring-like aggregations of organelles) was visualised using an NADH-TR stain.[6] This abnormality is poorly suited to automated quantification methods, so organelle mislocalisation was manually quantified by the Lead Pathologist at the time of initial biopsy evaluation and reported using previously established methods.[6,10] Briefly, biopsied tissue was photographed using a 20× objective on an Olympus BX53 microscope with the goal of documenting a minimum of 300 fibres in the image. The field selected for photography was judged to be an area with the highest degree of organelle mislocalisation in each specimen, and the suitability of selected fields was assessed by the Biopsy Review Committee during biopsy analysis. The image was quantified manually using the Cell Counter tool in ImageJ software, with respect to the number of fibres with appropriate organelle localisation or inappropriate organelle localisation, and these numbers were integrated into the biopsy report by the Lead Pathologist and used in overall grading.

XLMTM pathology score

An overall XLMTM pathology score previously developed for the preclinical canine studies[10] was used here in an attempt to summarise overall pathological severity. Briefly, the score is based on an estimate of the overall proportion of fibres in the biopsy displaying some key elements of characteristic XLMTM pathology (myofibre smallness, organelle mislocalisation, or internal nucleation). Grading was assigned as follows: Grade 0, no XLMTM pathology (normal muscle or muscle with scattered atrophic fibres); Grade 1, very mild XLMTM pathology (<10% of fibres with XLMTM pathology); Grade 2, mild XLMTM pathology (11–30% of fibres with XLMTM pathology); Grade 3, moderate XLMTM pathology (31–60% of fibres with XLMTM pathology); Grade 4, moderate/severe XLMTM pathology (61–80% of fibres with XLMTM pathology); and Grade 5, severe/very severe XLMTM pathology (≥81% of fibres with XLMTM pathology). To address the impact of participant's age on expected myofibre size, limited age group information was provided on biopsies to establish whether a given sample was from a child <2 years old, between 2 and 4 years old, or >4 years old. This allowed the recognition of myofibre smallness on samples without dramatic abnormalities in the variation of myofibre size to the extent that minFeret diameter median values of <11 μm were definitively abnormal for participants <2 years old, median values of <14 μm were definitively abnormal for participants 2–4 years old, and median values of <23 μm were definitively abnormal for participants >4 years old.[16]

Electron microscopy and quantification of sarcotubular structures

A longitudinally oriented portion of each biopsy was fixed in 2% glutaraldehyde + 4% paraformaldehyde in sodium cacodylate buffer, pH 7.4, and transferred to sodium cacodylate buffer after 2 h of fixation. Samples were shipped and processed for electron microscopy at the Medical College of Wisconsin Electron Microscopy Core Facility for evaluation of the number of transverse tubules (T-tubules), longitudinal tubules (L-tubules; structures with the ultrastructural appearance of T-tubules but oriented longitudinally), and triads as previously described.[10] Briefly, following standard processing, Epon-embedded tissue was sectioned at 70 nM in thickness and further stained with 2% uranyl acetate and Reynold's lead citrate. Electron microscopy was performed and photographed by the Core facility staff using a Hitachi H600 transmission electron microscope. Evaluation and quantitation were focused on longitudinally oriented myofibres, as these provide the best view of the sarcotubular organisation. Individual fibres were surveyed and the area of each fibre with the most appropriate orientation for sarcotubular visualisation was photographed at 10,000×, 20,000×, and 30,000× magnification, with only one area photographed per fibre. These photographs were provided to the Biopsy Review Committee for evaluation, and each individual pathologist reviewing the case conducted a count of T-tubules, L-tubules, and triads that are present in each 20,000× image. The other magnification images were not quantified but were provided for reference. Significant discrepancies between counts were discussed and resolved by consensus in online Biopsy Review Committee meetings.

Co-immunoprecipitation/western blot

Based on the increased p62 positivity seen in several post-treatment samples by immunofluorescence, a

focused experiment on the sample with greatest p62 positivity was performed to determine whether significant amounts of myotubularin were bound to p62 protein. A Pierce Co-IP kit (Thermo Scientific 26149) was used to perform the co-immunoprecipitation experiment. An anti-p62 antibody (P0067, rabbit, Sigma Aldrich) was used to immobilise the column of AminlLink plus Coupling Resin. 35 mg of muscle tissue from the 24 weeks biopsy on Participant 20 was used as an example of a treated XLMTM sample with increased p62 fluorescence signal at this timepoint. 35 mg of muscle tissue from a postmortem XLMTM tissue collection was used as a nontreated control condition. These muscle samples were lysed in ice-cold IP lysis buffer containing phosphatase and protease inhibitors, and lysates were pre-cleared by control agarose resin. Cleared lysates were added to p62 immobilised columns and mixed overnight at 4 °C. The columns were spun at 1000 × *g* and the flow-through was saved. p62 and the proteins bound to it were eluted in 50 µL of elution buffer.

To determine whether p62 was significantly bound to myotubularin following treatment, western blots were performed using protein isolates from tissue lysates (input) as well as the column flow-through and eluate from the coimmunoprecipitation procedure. These protein sources were used for SDS-PAGE western blot analysis using standard techniques.[8] Antibodies and conditions used are shown in Supplementary Table S2. Signals were detected by Clarity™ Western ECL Substrate (BIO-RAD 170-5061) and visualised with Chemidoc MP Imaging System.

Muscle biopsy evaluation

Portions of biopsy tissue were assessed for vector copy number, transgene mRNA expression, myotubularin protein expression, and tissue pathology. Procedures associated with clinical evaluation, safety, myotubularin expression, mRNA expression, anti-AAV8 neutralising antibodies, anti-myotubularin antibodies, and vector copy number analyses are published in detail.[11]

The Muscle Biopsy Review Committee consisted of expert paediatric skeletal muscle pathologists. The Lead Pathologist (MWL) reviewed and reported pathological findings using scanned slide images and a reporting template based on the NINDS Common Data Elements for Muscle Biopsy Reporting.[17] A minimum of two committee members reviewed each Lead Pathologist report. Instances of significant disagreement were resolved via consensus by at least two of the three reviewing committee members. Groups of biopsies evaluated together included at least one pre-treatment and one post-treatment sample in each reviewed group, and all biopsy evaluations were performed blinded with respect to patient ID, treatment status, and timepoint.

Pathological endpoints

Quantitative or semiquantitative pathological endpoints were based on nonclinical studies of AAV-MTM1 gene therapy in murine and canine models of XLMTM,[8,10,18] which displayed reversal of characteristic XLMTM findings including small myofibres, organelle mislocalisation, internally placed nuclei, and a loss of triad structures on electron microscopy. Detailed methods to measure myofibre size and type, quantify internally or centrally nucleated fibres and organelle mislocalisation, and determine XLMTM pathology score (as established in prior canine studies[10]) are described above. Ultrastructural features noted in XLMTM (e.g. numbers of T-tubules, L-tubules, and triads) were evaluated by electron microscopy, as described above.

Sample size estimation

The ASPIRO study followed an intent-to-treat principle. Of the 24 treated study participants in the ASPIRO trial, analysis for the pathology substudy was performed on all muscle biopsies corresponding to patients who had reached the 48-week biopsy timepoint at the time of analysis, with no exclusions due to protocol deviations. Therefore, no formal sample size or power calculations were performed.

Statistical analysis

Myofibre sizes were compared using a nonparametric Kolmogorov–Smirnov test of distribution equality. Within each participant, the distribution of myofibre sizes was compared in a pair-wise fashion between baseline, week 24, and week 48; where fibre sizes were compared multiple times within a patient, a Bonferroni multiple testing correction was applied to p-values to maintain a family-wise error rate of 0.05 within the statistical test. Analyses of other pathology outcomes were performed in all participants as a single group. Normality of each outcome was assessed using a Shapiro–Wilk normality test. Most outcomes were non-normally distributed; therefore, outcomes at baseline and week 48 were compared using a Wilcoxon sign rank test. The resulting p-values from these two comparisons were adjusted for multiple comparisons using the Bonferroni method to retain an overall type I error rate of 0.05. Analyses were performed with STATA V15 (College Station, TX) and a p-value $\leq$0.05 was considered statistically significant.

Ethics statement

The studies were conducted in accordance with International Conference on Harmonisation Good Clinical Practice guidelines, the Declaration of Helsinki, and guidance for the Clinical Investigation of Medicinal Products in the Pediatric Population. Study protocols were approved by the institutional review board of each institution. Signed informed consents were obtained

from participants' parent(s) or legal guardians. An independent data monitoring committee monitored the integrity and safety of the trial. Muscle biopsy studies were performed in accordance with the ethical standards of UCLA IRB Study #: IRB#17-000369-CR-00002, providing reliance oversight to the Medical College of Wisconsin.

Role of funders

This study was funded by Astellas Gene Therapies, formerly Audentes Therapeutics, Inc. Astellas Gene Therapies manufactured the investigational drug and designed and managed the trial. Employees/former employees of Astellas Gene Therapies who qualified as authors for this publication are included in the author byline; their contributions and disclosures are reported in the Contributors and Declaration of Interests sections, respectively. No authors received payment for writing this article. Medical writing support is reported in the Acknowledgements section and was funded by Astellas Gene Therapies. Authors were not precluded from accessing data in the study, and they accepted responsibility to submit for publication.

Results

Baseline demographic and clinical characteristics of all resamirigene bilparvovec-treated participants enrolled in the ASPIRO study (N = 24) are published elsewhere.[11] For the individuals included in the muscle biopsy study, baseline demographics and clinical characteristics are provided in Table 1: mean age at dosing was 1.7 years (range 0.8–4.1) in the lower-dose cohort (N = 6; Groups 1, 2) and 4.2 years (1.3–6.8 years) in the higher-dose Group 3 (N = 4) (Fig. 1). A summary of the treatment-emergent adverse events observed in the individuals included in this muscle biopsy study is presented in Supplementary Table S3.

Muscle sampling was successful in 28 of 30 attempted biopsies. In two biopsies (Participant 01, week 48 and Participant 02, week 24), specimens comprised fibrous and fatty tissue, with no skeletal muscle present. In Participant 02, who had poor muscle bulk in the lower extremity, the week-48 biopsy was performed in the triceps brachii after MRI imaging confirmed appropriate muscle bulk at that location.

Muscle biopsy findings are shown in parallel with selected demographic, clinical, and biochemical data that have been published separately (Figs. 2–4), as this allows contextualisation of the pathological findings to the status of the participant at the same timepoint. While myotubularin western blot data are also published separately, representative western blot images are included as Supplementary Figure S2 as evidence of target engagement.

Baseline biopsies from 8 of 10 participants showed similar pathological findings, despite the wide age range at biopsy (0.8–6.8 years) [Figs. 2–4]. H&E staining revealed myofibre size variation within samples due principally to the presence of numerous small fibres (Fig. 5, and Tables 2 and 3). Myofibre shape was normal or round, consistent with hypotrophy rather than atrophy as the reason for small size. There were also populations of large, round fibres in most biopsies. While the small fibre population included myofibres positive for slow, fast, foetal, and embryonic myosins, the larger fibre population was almost exclusively composed of fast fibres (Supplementary Figure S3). Centrally- and internally placed nuclei in myofibres were increased in number compared to normal muscle biopsies, and consistent with a classic appearance for XLMTM or other severe centronuclear myopathy (Fig. 6, Tables 2 and 3). NADH-TR stains revealed central aggregations of organelles, with subsarcolemmal areas of clearing in many fibres, also highly suggestive of XLMTM. The proportion of fibres with organelle mislocalisation was variable but high across all ten cases (Fig. 6, Tables 2 and 3). The histological appearance of two baseline biopsies (Participant 21 and Participant 02) were suggestive of more severe manifestation of the disease in comparison to the others. For Participant 21 (Fig. 3b), essentially all fibres showed severe myofibre smallness and organelle mislocalisation, without a subpopulation of larger fibres that was observed in all other baseline biopsies (Table 2). For Participant 02 (Fig. 4d), particularly severe pathological changes corresponded to an unusual level of fatty infiltration.

Post-treatment pathology findings were similar across subsets of participants receiving the same dose of resamirigene bilparvovec and immunosuppression. In Treatment Group 1, post-treatment biopsies showed staged recovery firstly of organelle localisation and then

Characteristic	1.3×10^{14} vg/kg (n = 6)	3.5×10^{14} vg/kg (n = 4)
Mean (SD) age at dosing, months	20.3 (16.5)	47.5 (28.9)
Mean (SD) weight, kg	11.7 (5.2)	16.7 (4.8)
Race, n (%)		
White	6 (100)	3 (75)
Asian	0	0 (0)
Black or African American	0	1 (25)
Functional classification of *MTM1* variants by predicted consequence on protein function, n (%)		
Loss of function	2 (33.3)	2 (50)
Partial loss of function	2 (33.3)	1 (25)
In-frame exonic deletion	2 (33.3)	1 (25)
Mean (SD) total CHOP INTEND score[a]	37.7 (5.9)	32.5 (6.0)
Mean (SD) ventilator dependence, hours per day	20.5 (5.0)	23.6 (0.8)
Mean (SD) MIP, cmH_2O	29.9 (10.0)	20.0 (10.7)

CHOP INTEND, Children's Hospital of Philadelphia Infant Test of Neuromuscular Disorders; MIP, maximal inspiratory pressure; SD, standard deviation. [a]Scores range 0–64, with higher scores indicating better function.

Table 1: **Demographic and clinical characteristics at baseline of the 10 dosed participants in the pathology substudy.**

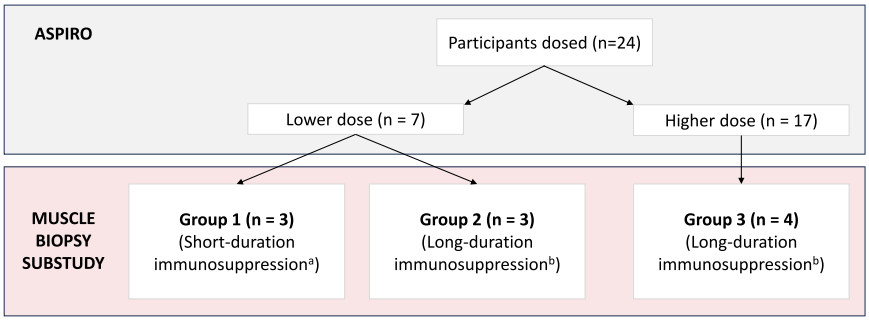

Fig. 1: **Resamirigene bilparvovec dosage level and duration of immunosuppression for the 10 participants analysed in the pathology substudy**. Muscle biopsy samples were collected at baseline (predose) and at weeks 24 and 48 following treatment with resamirigene bilparvovec gene therapy at either lower dose (1.3×10^{14} vg/kg) or higher dose (3.5×10^{14} vg/kg). [a]Prednisolone (1 mg/kg) administered for 4 weeks followed by a 4-week taper; [b]Prednisolone (1 mg/kg) administered for 8 weeks followed by an 8-week taper.

myofibre size over 48 weeks, accompanied by variable degrees of cellular infiltration. A readily apparent decrease in organelle mislocalisation on NADH-TR stains was observed from baseline to week 24 in all three participants (Figs. 2, 5 and 6, and Tables 2 and 3). Changes in fibre size were not visually apparent at week 24 although statistically significant differences were detected between baseline and week 24 due to the very large number of fibre measurements (Fig. 6).

The proportion of internally nucleated fibres at baseline was high in Group 1 (range 35–65%) and decreased to approximately 20% of fibres in all biopsies by week 24. Between 24 and 48 weeks post-treatment, there was an increase in myofibre size but essentially no further change in the proportion of internally nucleated myofibres (Fig. 6, Tables 2 and 3). A variable degree of cellular infiltration was observed in these three participants, with the most apparent cellular infiltrates (mild/moderate mixed cellular infiltrate with rare degenerating/regenerating myofibres) seen in Participant 17, minimal to no cellular infiltrates in Participant 08, and an intermediate degree of cellular infiltration in Participant 05 (Fig. 7). Of note, Participant 05 had been treated with additional immunosuppression therapies (mycophenolate mofetil, rapamycin, and intravenous immunoglobulin treatment) at or near the week-24 biopsy, the impact of which on cellular infiltration within the biopsy is uncertain. The cellular infiltrate was a mixture of lymphocytes (CD3+CD4+, CD3+CD8+, and more rarely CD20+), and macrophages (CD68+). Membrane attack complex (C5b-9) deposition was not observed in any post-treatment biopsy.

In Treatment Group 2, pathological findings in Participants 20 and 19 (Figs. 3, 5 and 6, and Tables 2 and 3) were similar to those in Group 1, but no cellular infiltration was observed. Again, there was a striking decrease from baseline to week 24 in organelle mislocalisation on NADH-TR stains. While changes in fibre size were not visually apparent at week 24, an evident increase in myofibre size was observed at week 48. Participant 21 showed more severe pathology at baseline (including myofibre smallness and organelle mislocalisation in most fibres) and a slightly different pattern of treatment-induced changes: fibre size and organelle localisation showed improvements at week 24, with little additional change at the week 48 biopsy (Tables 2 and 3). Internal/central nucleation in Group 2 was highly variable and did not correlate with clinical improvement.

The pathological response to treatment in Group 3 participants was highly variable (Figs. 4–6, and Tables 2 and 3). Three of 4 participants had biopsies at week 24 and showed similar decreases in organelle mislocalisation between baseline and week 24 as those observed in Groups 1 and 2. An apparent large increase in myofibre size in Participants 25 and 23 at week 24 suggested a more rapid pathological recovery than in the lower-dose groups and contributed to the decision made in conjunction with the Data Monitoring Committee at that time to use the 3.5×10^{14} vg/kg dose for the remainder of the study. Similar to Groups 1 and 2, week-48 biopsies also displayed myofibre growth. In addition, a mild focal lymphohistiocytic infiltrate was observed in the week-48 biopsy of Participant 23 (Fig. 7); this was associated with a few basophilic and embryonic myosin-positive fibres, consistent with active myofibre regeneration, despite being on rapamycin therapy at both week-24 and week-48 biopsies. For Participant 02, the week-48 biopsy displayed abnormal organelle localisation in 43% of fibres in comparison to 99% at baseline. Internal/central nucleation for Group 3 was highly variable and did not correlate with clinical improvement.

Only a subset of the histological features assessed demonstrated responsiveness to treatment. Treatment was associated with improvement of XLMTM pathology score over baseline levels (Fig. 6b, Table 3, Supplementary Table S4), although the magnitude of

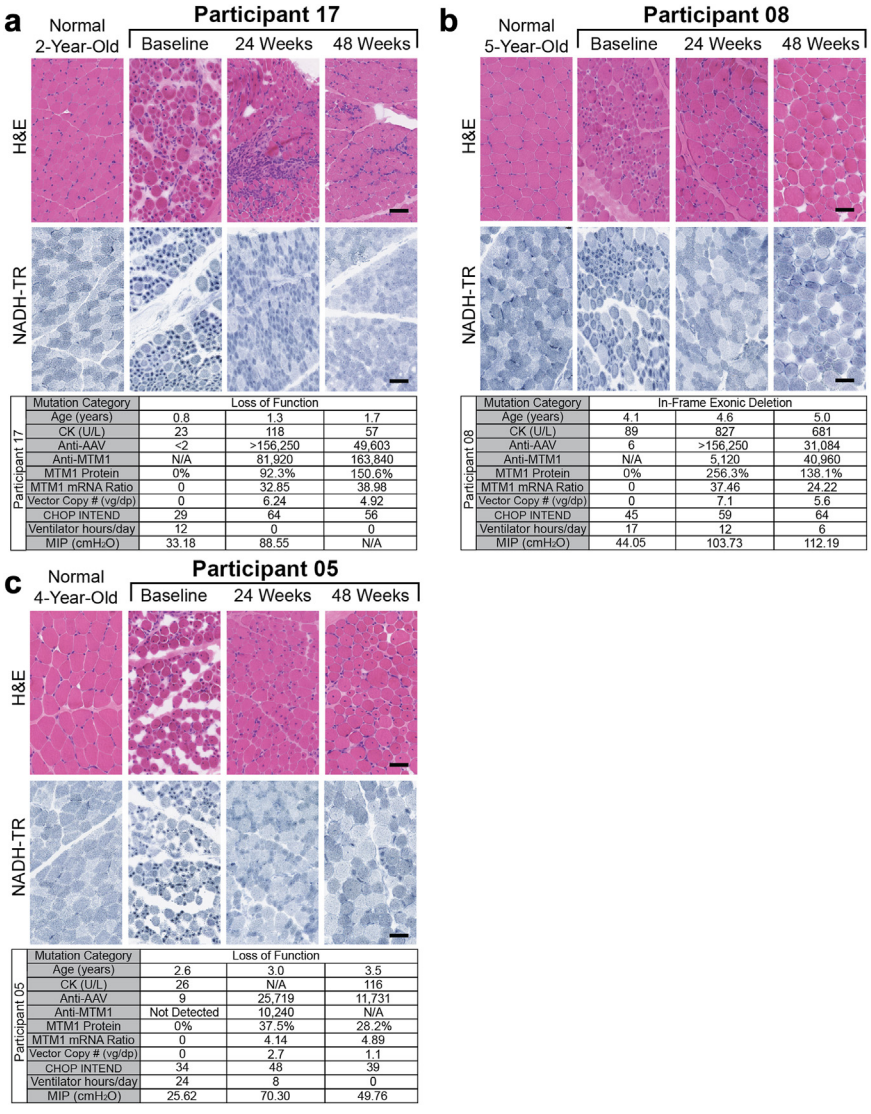

Participant 17	Mutation Category	Loss of Function		
	Age (years)	0.8	1.3	1.7
	CK (U/L)	23	118	57
	Anti-AAV	<2	>156,250	49,603
	Anti-MTM1	N/A	81,920	163,840
	MTM1 Protein	0%	92.3%	150.6%
	MTM1 mRNA Ratio	0	32.85	38.98
	Vector Copy # (vg/dp)	0	6.24	4.92
	CHOP INTEND	29	64	56
	Ventilator hours/day	12	0	0
	MIP (cmH_2O)	33.18	88.55	N/A

Participant 08	Mutation Category	In-Frame Exonic Deletion		
	Age (years)	4.1	4.6	5.0
	CK (U/L)	89	827	681
	Anti-AAV	6	>156,250	31,084
	Anti-MTM1	N/A	5,120	40,960
	MTM1 Protein	0%	256.3%	138.1%
	MTM1 mRNA Ratio	0	37.46	24.22
	Vector Copy # (vg/dp)	0	7.1	5.6
	CHOP INTEND	45	59	64
	Ventilator hours/day	17	12	6
	MIP (cmH_2O)	44.05	103.73	112.19

Participant 05	Mutation Category	Loss of Function		
	Age (years)	2.6	3.0	3.5
	CK (U/L)	26	N/A	116
	Anti-AAV	9	25,719	11,731
	Anti-MTM1	Not Detected	10,240	N/A
	MTM1 Protein	0%	37.5%	28.2%
	MTM1 mRNA Ratio	0	4.14	4.89
	Vector Copy # (vg/dp)	0	2.7	1.1
	CHOP INTEND	34	48	39
	Ventilator hours/day	24	8	0
	MIP (cmH_2O)	25.62	70.30	49.76

***Fig. 2:* Biopsy findings in Group 1 participants**. H&E and NADH-TR staining of biopsies from **(a)** Participant 17, **(b)** Participant 08, and **(c)** Participant 05 are shown. Participants in this group received lower-dose resamirigene bilparvovec (1.3×10^{14} vg/kg) and a short duration of immunosuppression (1 mg/kg of prednisolone for 4 weeks followed by a 4-week taper). A normal biopsy age-matched to each participant's 48-week biopsy is shown for comparison. Also shown are participant's age at the time of biopsy, serum creatine kinase (CK), quantification of serum anti-AAV antibodies and anti-myotubularin (anti-MTM1) antibodies taken at or near the time of the biopsy, the values for myotubularin protein (MTM1 protein, % of normal skeletal muscle), *MTM1* RNA, and vector copy number that were obtained from the biopsy tissue, CHOP INTEND score, hours per day of ventilator dependence at each of these timepoints, and maximal inspiratory pressure (MIP). Scale bar = 50 μm.

improvement was smaller than for other endpoints due to the persistence of internal nucleation in many biopsies. Endpoints including fibre type proportions (Table 3, Supplementary Figure S3), ultrastructural findings (Table 3, Supplementary Figure S4), and satellite cell number (Table 3, Supplementary Figure S5) did not display statistically significant alterations following treatment, and these results are discussed in more detail in the Supplementary Results. Evaluation of autophagy-related proteins (p62, LC3, LAMP2) identified aggregated material in baseline biopsies that was not observed in post-treatment biopsies, with an increase in cytoplasmic p62 in eight of ten week-24 biopsies (Supplementary Results, Supplementary Figure S6).

Discussion

The approach to muscle biopsy evaluation in the ASPIRO trial was adapted from work in murine and canine models of XLMTM,[8] which display similar

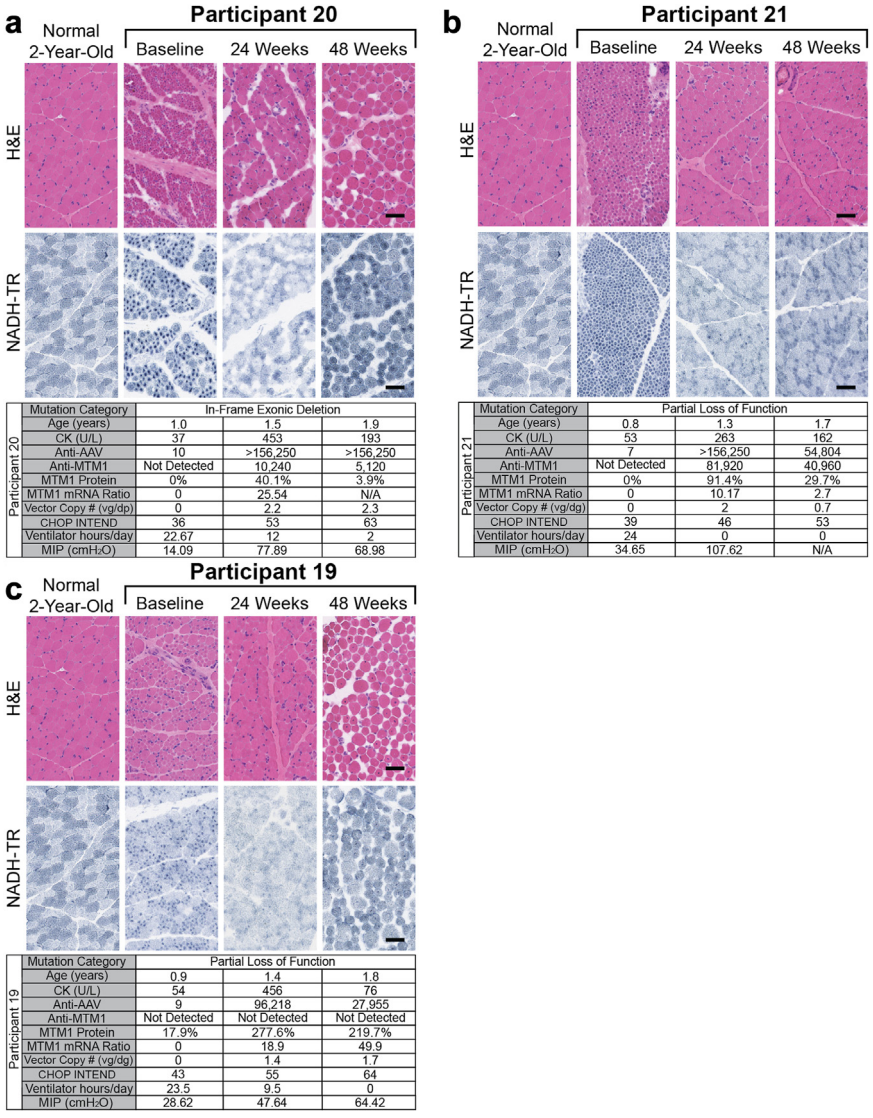

Participant 20	Mutation Category	In-Frame Exonic Deletion		
	Age (years)	1.0	1.5	1.9
	CK (U/L)	37	453	193
	Anti-AAV	10	>156,250	>156,250
	Anti-MTM1	Not Detected	10,240	5,120
	MTM1 Protein	0%	40.1%	3.9%
	MTM1 mRNA Ratio	0	25.54	N/A
	Vector Copy # (vg/dp)	0	2.2	2.3
	CHOP INTEND	36	53	63
	Ventilator hours/day	22.67	12	2
	MIP (cmH_2O)	14.09	77.89	68.98

Participant 21	Mutation Category	Partial Loss of Function		
	Age (years)	0.8	1.3	1.7
	CK (U/L)	53	263	162
	Anti-AAV	7	>156,250	54,804
	Anti-MTM1	Not Detected	81,920	40,960
	MTM1 Protein	0%	91.4%	29.7%
	MTM1 mRNA Ratio	0	10.17	2.7
	Vector Copy # (vg/dg)	0	2	0.7
	CHOP INTEND	39	46	53
	Ventilator hours/day	24	0	0
	MIP (cmH_2O)	34.65	107.62	N/A

Participant 19	Mutation Category	Partial Loss of Function		
	Age (years)	0.9	1.4	1.8
	CK (U/L)	54	456	76
	Anti-AAV	9	96,218	27,955
	Anti-MTM1	Not Detected	Not Detected	Not Detected
	MTM1 Protein	17.9%	277.6%	219.7%
	MTM1 mRNA Ratio	0	18.9	49.9
	Vector Copy # (vg/dg)	0	1.4	1.7
	CHOP INTEND	43	55	64
	Ventilator hours/day	23.5	9.5	0
	MIP (cmH_2O)	28.62	47.64	64.42

***Fig. 3*: Biopsy findings in Group 2 participants**. H&E and NADH-TR staining of biopsies from **(a)** Participant 20, **(b)** Participant 21, and **(c)** Participant 19 are shown. Participants in this group received lower-dose resamirigene bilparvovec (1.3×10^{14} vg/kg) and a long duration of immunosuppression (1 mg/kg of prednisolone for the first 8 weeks followed by an 8-week taper). A normal biopsy age-matched to each participant's 48-week biopsy is shown for comparison. Also shown are participant's age at the time of biopsy, serum creatine kinase (CK), quantification of serum anti-AAV antibodies and anti-myotubularin (anti-MTM1) antibodies taken at or near the time of the biopsy, the values for myotubularin protein (MTM1 protein, % of normal skeletal muscle), *MTM1* RNA, and vector copy number that were obtained from the biopsy tissue, CHOP INTEND score, hours per day of ventilator dependence, and maximal inspiratory pressure (MIP) at each of these timepoints. Scale bar = 50 μm.

pathological features to those seen in human XLMTM.[6] XLMTM mice and dogs treated with AAV-MTM1 at efficacious doses show essentially normal histology, without myofibre smallness, organelle mislocalisation, or excessive internal nucleation,[8,10] with pathological recovery observed within 8 weeks of treatment. In comparison, the histopathological recovery seen in muscle biopsies of the ASPIRO study participants was slower and less complete. While there was readily apparent improvement of organelle mislocalisation by 24 weeks and improvement of myofibre size by 48 weeks post-treatment, nuclear placement was extremely variable and even exceeded baseline values in some cases (Fig. 8). This more gradual pathological improvement may partially explain the relatively gradual course of clinical improvement compared to that reported in XLMTM mice and dogs.[8,10] Nevertheless, as early as 4 weeks after dosing, treated participants in

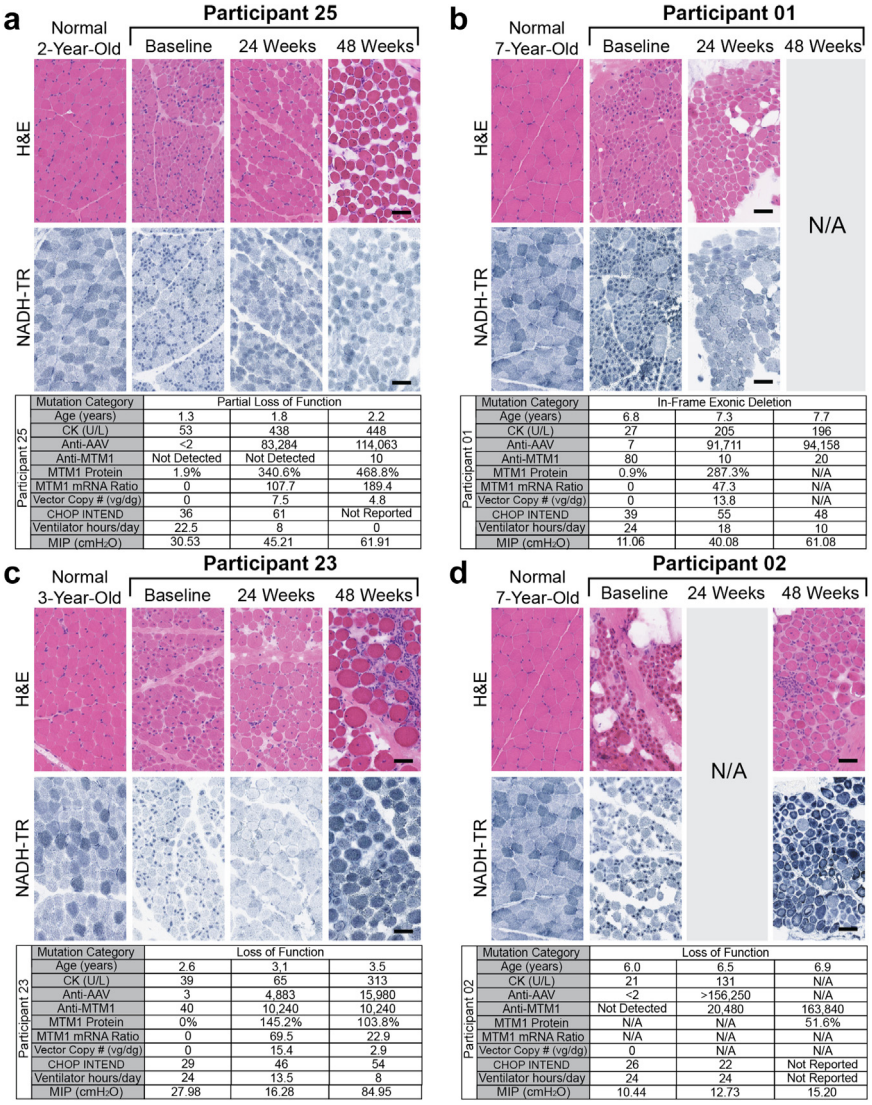

Participant 25

Mutation Category	Partial Loss of Function		
Age (years)	1.3	1.8	2.2
CK (U/L)	53	438	448
Anti-AAV	<2	83,284	114,063
Anti-MTM1	Not Detected	Not Detected	10
MTM1 Protein	1.9%	340.6%	468.8%
MTM1 mRNA Ratio	0	107.7	189.4
Vector Copy # (vg/dg)	0	7.5	4.8
CHOP INTEND	36	61	Not Reported
Ventilator hours/day	22.5	8	0
MIP (cmH_2O)	30.53	45.21	61.91

Participant 01

Mutation Category	In-Frame Exonic Deletion		
Age (years)	6.8	7.3	7.7
CK (U/L)	27	205	196
Anti-AAV	7	91,711	94,158
Anti-MTM1	80	10	20
MTM1 Protein	0.9%	287.3%	N/A
MTM1 mRNA Ratio	0	47.3	N/A
Vector Copy # (vg/dg)	0	13.8	N/A
CHOP INTEND	39	55	48
Ventilator hours/day	24	18	10
MIP (cmH_2O)	11.06	40.08	61.08

Participant 23

Mutation Category	Loss of Function		
Age (years)	2.6	3.1	3.5
CK (U/L)	39	65	313
Anti-AAV	3	4,883	15,980
Anti-MTM1	40	10,240	10,240
MTM1 Protein	0%	145.2%	103.8%
MTM1 mRNA Ratio	0	69.5	22.9
Vector Copy # (vg/dg)	0	15.4	2.9
CHOP INTEND	29	46	54
Ventilator hours/day	24	13.5	8
MIP (cmH_2O)	27.98	16.28	84.95

Participant 02

Mutation Category	Loss of Function		
Age (years)	6.0	6.5	6.9
CK (U/L)	21	131	N/A
Anti-AAV	<2	>156,250	N/A
Anti-MTM1	Not Detected	20,480	163,840
MTM1 Protein	N/A	N/A	51.6%
MTM1 mRNA Ratio	N/A	N/A	N/A
Vector Copy # (vg/dg)	0	N/A	N/A
CHOP INTEND	26	22	Not Reported
Ventilator hours/day	24	24	Not Reported
MIP (cmH_2O)	10.44	12.73	15.20

Fig. 4: **Biopsy findings in Group 3 participants**. H&E and NADH-TR staining of biopsies from **(a)** Participant 25, **(b)** Participant 01, **(c)** Participant 23, and **(d)** Participant 02 are shown. Participants in this group received higher-dose resamirigene bilparvovec (3.5×10^{14} vg/kg) and a long duration of immunosuppression (1 mg/kg of prednisolone for the first 8 weeks followed by an 8-week taper). Note the 48-week biopsy for Participant 9 and the 24-week biopsy for Participant 12 are not shown because they did not contain muscle tissue. A normal biopsy age-matched to each participant's 48-week biopsy is shown for comparison. Also shown are participant's age at the time of biopsy, serum creatine kinase (CK), quantification of serum anti-AAV antibodies and anti-myotubularin (anti-MTM1) antibodies taken at or near the time of the biopsy, the values for myotubularin protein (MTM1 protein, % of normal skeletal muscle), *MTM1* RNA, and vector copy number that were obtained from the biopsy tissue, CHOP INTEND score, hours per day of ventilator dependence, and maximal inspiratory pressure (MIP) at each of these timepoints. For Participant 02, poor muscle bulk resulted in a lack of muscle tissue in the week 24 and necessitated a change in biopsy site to the triceps brachii for the week 48 biopsy. In addition, NADH-TR staining of the week 48 biopsy on Participant 02 reveals the persistence of XLMTM-type organelle mislocalisation in some fibres, in addition to a subsarcolemmal aggregation of organelles that is not observed in any other study specimens. Scale bar = 50 μm.

ASPIRO demonstrated clinically meaningful improvements in motor function, as measured on the Children's Hospital of Philadelphia Infant Test of Neuromuscular Disorders (CHOP INTEND) and noticeable improvements in respiratory strength (maximal inspiratory pressure; MIP).[11] Over the course of follow-up, at 48-weeks and up to the reported 28 February 2022 data-cut, most participants continued to improve clinically and achieved functional outcomes such as reduced ventilator dependence, and ability to sit, stand and walk,

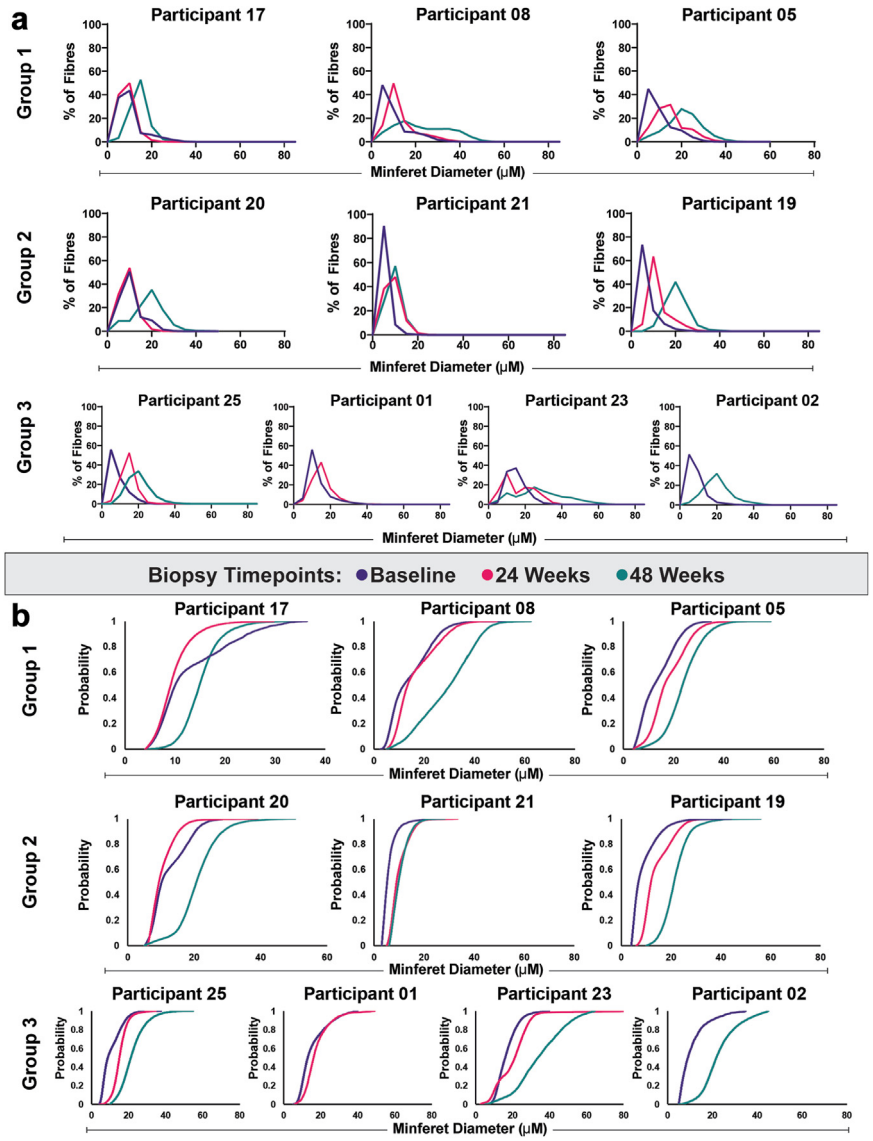

Fig. 5: **Detailed myofibre size information**. Myofibre size measurements were obtained and plotted using **(a)** frequency histogram and **(b)** cumulative probability plot methods. Due to the very large numbers of fibres sampled, all comparisons between all timepoints in a given participant demonstrated statistically significant differences at a level of $p < 0.001$ (nonparametric Kolmogorov–Smirnov test of distribution equality).

which are unprecedented in chronically ventilated individuals with a congenital myopathy.[11]

This substudy offered a valuable opportunity to evaluate XLMTM disease pathology at a variety of ages, and this was unique because most diagnostic biopsies for XLMTM occur within the first few months of life. Surprisingly, we found little difference in the appearance of XLMTM biopsies taken at <1 year of age in comparison to those taken after several years, which suggests an arrest of growth in most myofibres after the first few months of life. This likely does not correspond to a "developmental arrest" as mature myosin isoforms are detected in most fibres, but the disease process does limit myofibre growth and this limitation does not appear to be affected by age. Thus, it is worth noting that all participants appear to have been treated at a timepoint where XLMTM-related pathology was consistently present, and the age of treatment most likely impacted the difference between the observed histological findings and what would be normal for age. With respect to the degree of myofibre smallness for age, our findings helped identify how the current normal range of

Participant number	Timepoint (weeks)	MinFeret diameter (µm)		XLMTM-type organelle mislocalisation (%)	Punctate mislocalisation (%)	Internal/ central nucleation (%)
		50th Percentile	75th Percentile			
Group 1						
17	0	8	11	78	0	43
	24	8	10	0	13	19
	48	14	16	0	5	14
08	0	8	12	70	0	35
	24	11	15	0	2	23
	48	21	33	0	4	8
05	0	8	13	71	0	65
	24	14	19	0	20	21
	48	21	26	0	17	26
Group 2						
20	0	9	12	83	0	33
	24	9	11	0	11	20
	48	19	23	0	36	34
21	0	5	6	83	0	32
	24	8	10	3	4	7
	48	9	11	0	2.5	7
19	0	6	8	72	0	13
	24	11	13	0	16	12
	48	20	23	0	18	24
Group 3						
25	0	7	10	68	0	20
	24	14	16	0	5	9
	48	19	24	0	31	38
01	0	11	15	76	0	36
	24	15	18	0	4	17
	48	[a]	[a]	[a]	[a]	[a]
23	0	14	18	63	0	35
	24	13	22	0	12	28
	48	27	37	0	23	19
02	0	7	10	99	0	35
	24	[a]	[a]	[a]	[a]	[a]
	48	20	24	21	3.2	24

Fibre size is shown in reference to the values of the 50th percentile and the 75th percentile of maximum fibre size on each biopsy. With the exception of the biopsy from Participant 02, organelle mislocalisation corresponded to one of two patterns; 1) a dense aggregation of organelles that is characteristic of untreated XLMTM ("XLMTM-type") or 2) smaller, punctate aggregates (often associated with nuclei) that are abnormal but are not characteristic of XLMTM. The biopsy from Participant 02 had an additional component of subsarcolemmal organelle mislocalisation, the significance of which is unclear. The percentage of internally nucleated fibres (including centrally nucleated fibres) is also shown. [a]No muscle for assessment. XLMTM, X-linked myotubular myopathy.

Table 2: **Individual values of key light microscopic endpoints on each muscle biopsy.**

myofibre size values (which is based on studies of a small number of patients scattered across the paediatric age range) is insufficient for the evaluation of clinical trial data. Our group has coordinated a multicentre study of 349 non-XLMTM patient biopsies to establish more robust fibre size norms for children, and this will be published separately in the near future. For the purpose of contextualising data in this study, we can state that the mean myofibre minFeret diameter for boys at age 1 year is 15.6 µm, at age 2 is 22.2 µm, at age 3 is 23.5 µm, at age 4 is 27.3 µm, at age 5 is 29.9 µm, and at age 7 is 33.2 µm. Comparing the study findings from resamirigene bilparvovec-treated participants in ASPIRO to these values illustrates the degree of myofibre smallness at baseline and the degree to which recovery is occurring in the post-treatment biopsies. Cellular infiltration of the target tissue is a recognised effect of AAV-based gene therapy and an important consideration in clinical trials.[13] A recent study has shown that cellular infiltrates in rAAV-injected muscles could be regulatory cells, rather than cytotoxic cells,[19,20] so it is possible that cellular infiltration in some samples does not constitute an inflammatory response. Mixed lymphohistiocytic infiltrates were observed in the post-treatment biopsies of five participants in our study, in both dose groups and at either biopsy timepoint; in

Assessment	Timepoint (weeks)	Group 1		Group 2		Group 3		All Groups	
		Median (95% CI)	N	Median (95% CI)	N	Median (95% CI)	N	Median (95% CI)	N
MinFeret Diameter 50th Percentile (μm)	0	8 (8–8)	3	6 (5–9)	3	9 (4–17)	4	8 (7–10)	10
	24	11 (8–14)	3	9 (8–11)	3	14 (13–15)	3	11 (9–14)	9
	48	21 (14–21)	3	19 (9–20)	3	20 (19–27)	3	19 (16–22)	9
MinFeret Diameter 75th Percentile (μm)	0	12 (11–13)	3	8 (6–12)	3	13 (10–18)	4	12 (9–13)	10
	24	15 (10–19)	3	11 (10–13)	3	18 (16–22)	3	15 (11–19)	9
	48	26 (16–33)	3	23 (11–23)	3	24 (24–37)	3	25 (19–28)	9
XLMTM-Type Organelle Mislocalisation (%)	0	71 (70–78)	3	83 (72–83)	3	72 (63–99)	4	77 (73–79)	10
	24	0 (0–0)	3	0 (0–3)	3	0 (0–0)	3	0 (0–1)	9
	48	0 (0–0)	3	0 (0–0)	3	0 (0–21)	3	0 (0–7)	9
Internal/Central Nucleation (%)	0	43 (35–65)	3	32 (13–33)	3	35 (20–36)	4	31 (26–48)	10
	24	21 (19–23)	3	12 (7–20)	3	17 (9–28)	3	18 (13–21)	9
	48	14 (8–26)	3	24 (7–34)	3	24 (19–38)	3	22 (16–27)	9
Punctate Mislocalisation (%)	0	0 (0–0)	3	0 (0–0)	3	0 (0–0)	4	0 (0–0)	10
	24	13 (2–20)	3	11 (4–16)	3	5 (4–12)	3	10 (7–12)	9
	48	5 (4–17)	3	18 (3–36)	3	23 (3–31)	3	19 (9–19)	9
T Tubules (Count per 20,000× Field)	0	3 (2–4)	3	8 (3–8)	3	6 (1–9)	4	6 (3–6)	10
	24	7 (5–8)	3	6 (2–7)	3	8 (4–12)	3	6 (5–8)	9
	48	8 (7–9)	3	10 (7–17)	3	6 (5–7)	3	8 (6–11)	9
L Tubules (Count per 20,000× Field)	0	1 (0–1)	3	0 (0–1)	3	0 (0–1)	4	0 (0–1)	10
	24	0 (0–1)	3	1 (0–1)	3	0 (0–1)	3	0 (0–1)	9
	48	1 (0–1)	3	0 (0–0)	3	0 (0–1)	3	0 (0–0)	9
Triads (Count per 20,000× Field)	0	4 (3–4)	3	8 (4–8)	3	6 (1–10)	4	6 (4–7)	10
	24	7 (5–8)	3	6 (3–7)	3	9 (5–13)	3	7 (6–9)	9
	48	9 (8–9)	3	10 (8–17)	3	7 (6–7)	3	9 (7–11)	9
Pathology Score	0	4 (4–4)	3	5 (4–5)	3	5 (4–5)	4	5 (4–5)	10
	24	4 (4–5)	3	4 (3–4)	3	4 (2–5)	3	4 (4–4)	9
	48	2 (2–3)	3	3 (2–4)	3	3 (3–3)	3	3 (2–3)	9
Pax7 Fibres (%)	0	13 (5–17)	3	4 (4–4)	3	4 (4–7)	4	5 (4–12)	10
	24	9 (7–9)	3	5 (5–5)	3	7 (5–9)	3	7 (5–8)	9
	48	7 (6–11)	3	5 (8–5)	3	14 (11–20)	3	8 (6–15)	9
Slow Fibres (%)	0	80 (74–84)	3	83 (76–100)	3	81 (58–94)	4	79 (78–86)	10
	24	81 (67–85)	3	74 (72–76)	3	69 (49–96)	3	74 (71–78)	9
	48	80 (71–90)	3	73 (66–75)	3	88 (88–97)	3	80 (71–91)	9

Data were not normally distributed and are shown as the median and 95% confidence interval (CI). Note that statistical comparisons of these data shown in Fig. 6 were made by evaluating all biopsies together and statistics were not performed on separate groups.

Table 3: **Quantification of key pathological endpoints.**

some cases this was associated with rare degenerating and regenerating myofibres. This cellular infiltration and myofibre degeneration had not been observed in any study of AAV-MTM1 in mice, canines, or monkeys.[8,10] The cellular infiltrate comprised principally CD3+CD4+ or CD3+CD8+ T lymphocytes, and CD20+ B lymphocytes were only observed in areas of lymphocytic aggregation. CD68+ macrophages were scattered across areas with and without significant lymphocytic infiltration and were also observed in biopsies that did not display significant cellular infiltration in this study, but their function here is unclear. With respect to the humoral immune system, there was no deposition of C5b-9 on myofibre sarcolemmal surfaces in any biopsy, despite the presence in serum of high anti-AAV8 neutralising antibody titres starting at a few weeks post-treatment and of detectable anti-myotubularin antibody titres starting several months post-treatment.[11]

There are likely two factors that contributed to the presence and degree of cellular infiltration in some participants. Firstly, participants in Group 1 received the shorter course of corticosteroids and exhibited up to a mild/moderate degree of inflammation, while only mild or no cellular infiltration was observed in Group 2 and 3 participants in whom corticosteroid treatment duration was longer. This suggests that immunosuppression in the immediate post-treatment period has long-lasting positive effects on cellular infiltrates in tissue.

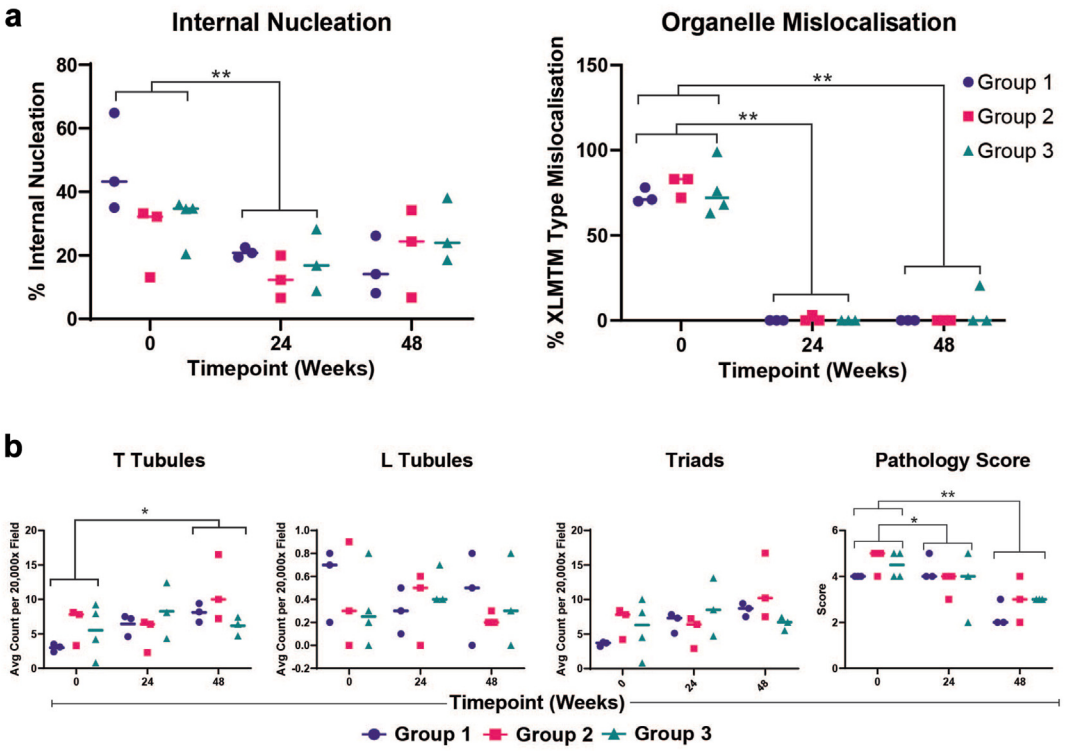

Fig. 6: **Quantification of key pathological endpoints**. **(a)** Quantification of internal nucleation (left) and organelle mislocalisation characteristic of XLMTM (right). Findings are shown for all individual participants within each group, and groups are distinguished by colour. **(b)** Individual participant data with respect to T-tubules, L-tubules, triads, and pathology score[a]. *p < 0.05, **p < 0.01 (Wilcoxon ranked test with the significance level set at p < 0.05). Note that statistical comparisons were made between time points by evaluating all biopsies together at each time point, and statistics were not performed on separate groups. [a]XLMTM pathology score grading was assigned as follows: Grade 0, no XLMTM pathology (normal muscle or muscle with scattered atrophic fibres); Grade 1, very mild XLMTM pathology (<10% of fibres with XLMTM pathology); Grade 2, mild XLMTM pathology (11–30% of fibres with XLMTM pathology); Grade 3, moderate XLMTM pathology (31–60% of fibres with XLMTM pathology); Grade 4, moderate/severe XLMTM pathology (61–80% of fibres with XLMTM pathology); and Grade 5, severe/very severe XLMTM pathology (>81% of fibres with XLMTM pathology).

Secondly, four of the five participants showing cellular infiltration have loss-of-function mutations and have therefore never been exposed to myotubularin protein prior to the gene therapy, a possible risk factor for immune-mediated allograft rejection-type cellular infiltration in the muscle. Participants with loss-of-function mutations will be closely assessed for inflammatory reactions as studies continue, and more aggressive approaches to immunosuppression may be useful in such cases. Some individuals with missense mutations also have undetectable myotubularin protein levels; therefore, the proportion of those without prior immune exposure to myotubularin may be higher than one would predict based on mutation. Finally, it should be noted that observation of cellular infiltrates on muscle biopsy correlated poorly with clinical efficacy and safety endpoints. Participant 17 had the highest anti-myotubularin antibody titres in the study, and yet displayed substantial recovery of motor and respiratory strength post-treatment.[11] Biopsies with the most severe cellular infiltration (such as Participant 17, week 24) were taken at times during which the participant was clinically well and when creatine kinase levels were not elevated. In contrast, the week-24 biopsy for Participant 08 had minimal cellular infiltration despite elevated creatine kinase levels at that time. Importantly, the presence of cellular infiltrates was not associated with lower myotubularin protein levels at any post-treatment timepoint, suggesting that signs of cellular infiltrates in muscle in the absence of other clinical indicators of muscle damage should be interpreted with caution. If the cellular infiltrates in some patients correspond to regulatory cells (regulatory or exhausted T cells) rather than cytotoxic cells,[19,20] one would not expect to see creatine kinase increases in association with cellular infiltration. Conversely, the findings could be consistent with low levels of myofibre damage that are insufficient to cause myonecrosis and inflammatory response. Most participants in this substudy displayed modest increases in creatine kinase after treatment that likely corresponds

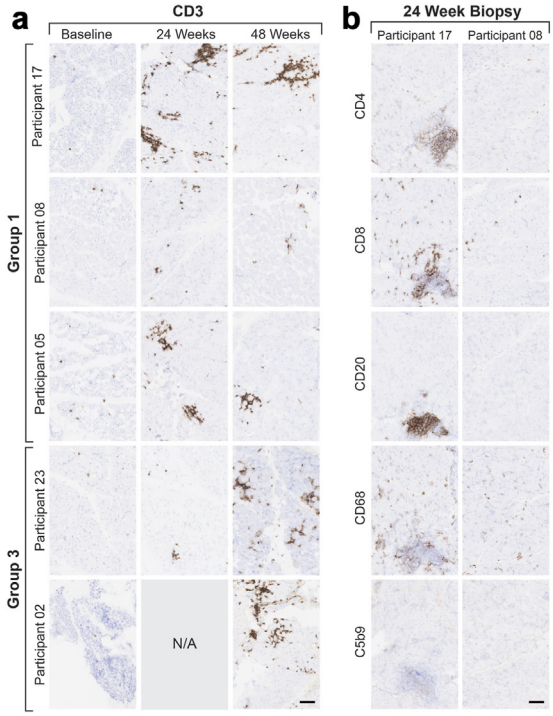

Fig. 7: **Evaluation of inflammation in muscle biopsies.** **(a)** CD3 staining of biopsies from study participants in which inflammation was noted at any timepoint demonstrates the relative degree of inflammation observed in individual biopsies. Any participants that are not shown did not have inflammation in any of the biopsies (Note that the 24-week biopsy for Participant 02 could not be evaluated due to lack of muscle tissue.) Scale bar = 50 μm. **(b)** Comparison of inflammatory markers in the 24-week muscle biopsies from Participants 17 and 08. Participant 17 showed the most inflammation overall in the study at this timepoint, despite low creatine kinase levels. Participant 08 showed very little inflammation while showing the highest creatine kinase in the study at this timepoint. Note that CD3 is a marker of T cells, CD4 is a marker of helper T (T_H) cells, CD8 is a marker of cytotoxic T (T_C) cells, CD20 is a marker of B cells, CD68 is a marker of macrophages, and C5b9 is a marker for the membrane attack complex of the complement cascade. Scale bar = 50 μm.

to some degree of muscle damage following treatment (especially for those with creatine kinase levels >300). While increases in creatine kinase can be observed during muscle growth and with increased muscle use, these factors would not explain the creatine kinase levels in the study participants who experienced the greatest post-treatment elevations. At this early stage, it remains unclear whether pathological or serum indicators of myofibre damage are helpful in clinical decision making or predictive of long-term efficacy.

Obtaining useful muscle biopsy material from young children with severe muscle disorders is challenging, as we experienced with two attempted biopsies that failed to yield viable muscle tissue, and observation of extensive fatty replacement in a third. This highlights the need to consider alternative biopsy sites for subsequent timepoints to maximise the chances of obtaining an adequate muscle sample, as was done for Participant 02 at week 48. In addition, the use of muscle MRI was a successful approach to identify an adequate muscle for obtaining a high-quality sample. In fact, the baseline biopsy for Participant 02 showed an unusual degree of muscle loss for a child of that age with XLMTM, and his week-48 biopsy showed unusual patterns of mitochondrial aggregation suggestive of additional muscle pathology beyond XLMTM. This participant did not experience significant functional recovery following treatment, unlike other participants described here, and he is undergoing further diagnostic testing in an effort to identify additional disease processes.

Additional limitations of this study include 1) the small sample size, 2) the inability to include a control group, 3) the potential for sampling issues to affect the detection of pathological findings, and 4) the inability to immunostain for myotubularin in tissue sections. With respect to sample size, the sample number is limited but this was mitigated by the consistency of pathological findings across patients. The pathological findings observed in baseline biopsies were similar in nearly all patients, and the impact of therapy on some endpoints (organelle mislocalisation, fibre size) were clear. If the baseline pathology or the pathological response to therapy were more heterogeneous, a much larger study might have been required to identify treatment-related pathological improvements. Although it is thought that the nonparametric Kolmogorov–Smirnov test used to compare myofibre size has relatively low power to test the null hypothesis, it is very sensitive to deviations from the null at high sample sizes. Hence, we sampled large numbers of fibres in each distribution to increase the sensitivity of the test. With respect to the lack of a control group for histology, it was not judged to be ethical to obtain biopsies from untreated XLMTM patients for the purpose of control comparisons. XLMTM is a severe disorder where surgical procedures and anaesthesia pose a significant potential health risk. Given the well-characterised disease pathology in XLMTM and the opportunity to obtain and analyse baseline biopsies from ASPIRO participants, the pursuit of control biopsies was not judged to be worth the risk that their collection would pose to patients. With respect to the potential for pertinent pathological changes to be missed due to the small size of the muscle samples and the patchy nature of some pathological processes, it is possible that some pathological findings discussed here (such as the presence of cellular infiltrates) were only patchily present in the muscle and may have been under- or over-sampled in the muscle biopsies. We do not believe that sampling affected the key XLMTM-related pathological findings (fibre size, organelle mislocalisation); however, as these findings were seen fairly

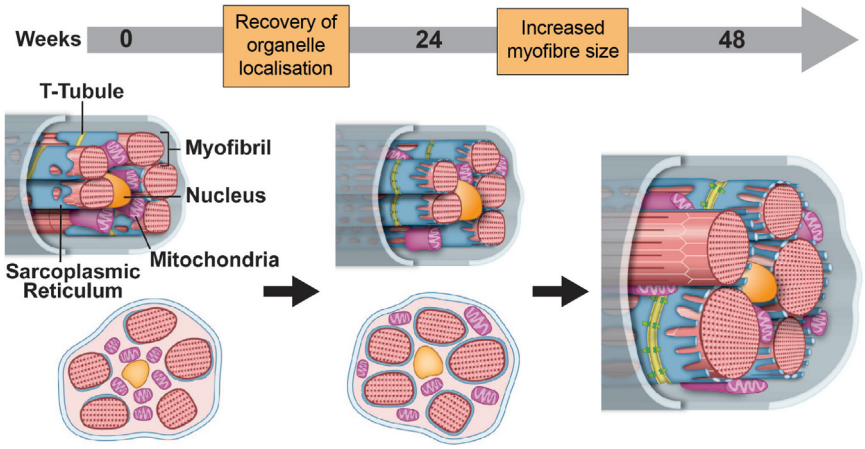

Fig. 8: **Summary of key structural changes following treatment with resamirigene bilparvovec**. Key elements of XLMTM pathology visible on light microscopy include small myofibre size, central aggregations of organelles, and internally placed nuclei (top). The earliest light microscopic improvement seen in all participants was restoration of appropriate organelle localization, in many cases without an impact on fibre size or nuclear placement (middle). By 48 weeks post-treatment, organelle localization remained appropriate and myofibre size had markedly increased. Nuclear placement was variable in post-treatment biopsies and in many cases did not improve with treatment.

uniformly across baseline biopsies in the study patients, the disease pathophysiology is not thought to occur focally. Lastly, the inability to establish a sensitive immunostaining assay for myotubularin posed some limitations in this study, as it would have been highly desirable to identify the localisation of treatment-related myotubularin protein and correlate this to pathological recovery. Unfortunately, after testing >40 anti-myotubularin antibodies, we were unable to identify an antibody that provided a positive signal in myotubularin-expressing conditions and an appropriately negative signal in myotubularin-null conditions in mouse and human tissue. The issue was mainly due to positive signal detected in myotubularin-null tissues, which is likely related to the binding of myotubularin-related (MTMR) proteins in muscle.

Muscle biopsies from ten boys with XLMTM dosed with resamirigene bilparvovec displayed significant changes to organelle localisation and myofibre size at timepoints coinciding with significant clinical improvements in muscle strength and respiratory function. Specifically, clinically important functional improvements were observed within the first 6 months after treatment, the time period in which only organelle localisation is uniformly improving in muscle biopsies. These findings shed new light on the predominant structural causes of muscle weakness in XLMTM and provide further context for the lack of functional improvements observed in animal studies where fibre size was improved without myotubularin restoration.[21] Additionally, the findings suggest that abnormal nuclear placement plays a minor role in the weakness observed in XLMTM. A limitation of this study is that long-term histopathological changes have not been characterised. Anecdotally, many of the study participants continue to attain motor milestones after the window when post-treatment biopsy specimens were collected, and it is not known whether some of the pathologic features of XLMTM are further improved at a later time.

It should be noted that serious adverse events (SAEs) have been observed in ASPIRO study participants,[11] including participants presented in this report (Supplementary Table S3), but that these safety events did not affect muscle biopsy pathology. The most common adverse events reported in the ASPIRO study were pyrexia, increases in creatine phosphokinase, and respiratory tract infections.[11] Of particular concern is the severe cholestatic liver dysfunction observed in the four boys that died (three at the 3.5×10^{14} vg/kg dose and one at the 1.3×10^{14} vg/kg dose) but who were not among the ten participants presented here.[12,22] Since the ASPIRO study, pre-existing cholestatic liver disease has been described in many patients with XLMTM and has been recognised as a clinical feature of the disease.[23–26] The ASPIRO study is paused while investigations are ongoing into cholestatic predilection in patients with XLMTM as well as the mechanisms by which resamirigene bilparvovec exacerbates this condition. While there were post-treatment observations of cellular infiltrates in muscle biopsies of some of the participants with XLMTM observed in the present report, no significant cellular infiltrates were observed in any liver biopsy or autopsy tissues analysed from the four fatalities; results from the investigations of these fatal SAEs will be presented in a separate report (manuscript under development). Further understanding of pathology in this rare disease, both muscle and non-muscle

manifestations alike, may help to inform future gene therapy strategies in XLMTM.

Contributors

MWL, SP, and SR designed the study. MWL, MB, PK, and HM provided study site/PI training. PK established and maintained regulatory practices, coordinated muscle biopsy collection, and performed quality assessments. MWL was lead pathologist of the muscle biopsy review committee, and BS (Schoser), MM, CAS, and KJ were members of the muscle biopsy review committee, which was responsible for slide review and planning of follow-up experiments. PBS, NLK, BKS, JJD, WM-F, CGB, AS, AB, SN, ARF, DNS, ET, and URQ coordinated muscle biopsy collection from study participants and summarised clinical data. SNK designed analytical tools. SD, HM, and MVA performed key experiments related to histology and autophagy. CW performed the electron microscopy experiments. MJP and EO performed data analysis related to histology and fibre size measurement. HG-D did the statistical analysis of fibre size data. MWL, MB, SNK, AHB, JL, CS, and FV were involved in data analysis/review and planning of follow-up experiments. MWL, SNK, and MB contributed to figure design. EC and WM provided overall study oversight and planning of follow-up work. SC provided clinical operations coordination and oversight. ESJ was involved in study operations and medical affairs coordination and oversight. SP and SR were involved in study planning and oversight and planning of follow up work. BS (Sepulveda) provided publication operations and medical affairs coordination and oversight. MWL wrote the first draft of the manuscript. All authors participated in the drafting and revision of the manuscript and have approved and consented for the submission of the final version. The following authors have accessed and verified the data reported in the manuscript: MWL, FV.

Data sharing statement

Researchers may request access to anonymised participant level data, trial level data and protocols from Astellas sponsored clinical trials at AGT_medinfo@astellas.com. For the Astellas criteria on data sharing see: https://clinicalstudydatarequest.com/Study-Sponsors/Study-Sponsors-Astellas.aspx.

Declaration of interests

MWL has received research funding from Astellas Gene Therapies* to his academic institution (Medical College of Wisconsin) and to his company (Diverge Translational Science Laboratory) for work related to the present manuscript; has received research grants or contracts to his academic institution (Medical College of Wisconsin) from Solid Biosciences, Kate Therapeutics, Taysha Therapeutics, Ultragenyx, and Prothelia; has received consulting fees from Astellas Gene Therapies*, Encoded Therapeutics, Modis Therapeutics, Lacerta Therapeutics, AGADA Biosciences, Dynacure, Affinia, Voyager, BioMarin, Locanabio, and Vertex Pharmaceuticals; has received speaker fees and reimbursement for travel related to sponsored research from Astellas Gene Therapies*; has received personal fees for scientific advisory board participation for Astellas Gene Therapies* and Solid Biosciences, and his institution has received payment from Taysha Therapeutics for his advisory board participation; he is currently CEO, founder, and owner of Diverge Translational Science Laboratory, which continues to work under contracts from many gene therapy companies including Astellas Gene Therapies*, Solid Biosciences, Rocket Pharma, Kate Therapeutics, Carbon Biosciences, Dynacure, Nationwide Children's Hospital, Taysha Gene Therapies, and Ultragenyx. BS (Schoser) has received grants/contracts, honoraria, and support for attending meetings from Astellas Gene Therapies* has participated in Advisory Boards for Dynacure. MM has received personal fees and study funding to her institution from Astellas Gene Therapies* in relation to the present manuscript. CAS has received royalties from Elsevier for the book "Muscle Biopsy. A Practical Approach". KAJ has received consulting fees from Astellas Gene Therapies* in relation to the present manuscript and other activities. PBS has received research funding from Astellas Gene Therapies* to support clinical trial investigations relating to the present manuscript; has received research contracts from Biogen, Dyne, Fulcrum, Pfizer, PTC Therapeutics, Reveragen, Sanofi, Sarepta, and Solid Biosciences; has received consulting fees from Alexion, Argenx, Biogen, Novartis Gene Therapies, Pfizer, UCB, and Sarepta; has received honoraria for lectures or presentations from Alexion, Argenx, Biogen, Catalyst, CSL Behring, Genentech, and Grifols; and has participated on Independent Data Monitoring Committees for Encoded Therapeutics, Excision BioTherapeutics, and Taysha. NLK reports research grants paid to her institution from AMO Pharma, Argenx, Astellas Gene Therapies*, Biogen, Biohaven, Novartis, NS Pharma, Sarepta, Reveragen, Roche, and Scholar Rock; has received payment for educational presentations from Sarepta; and has participated in a Data Safety Monitoring Board for Sarepta and Advisory Boards for Argenx, BioMarin, Fibrogen, Roche, and Sarepta. BKS has received institutional research grants or contracts to serve as an INCEPTUS and ASPIRO study site from Astellas Gene Therapies*. JJD has received research grants from NIH, CIHR, and Astellas Gene Therapies*; has received support for attending annual meetings from the World Muscle Society (as Executive Board Member) and TREAT NMD (as Chair of Executive Board); and receives annual honoraria as a Scientific Advisory Board member for the RYR1 Foundation. WMF has received support for study materials and study personnel relating to the present manuscript from Astellas Gene Therapies*; consulting fees from Sarepta, PTC Therapeutics, Novartis, and Roche; personal compensation from Novartis and Biogen, and institutional funding from Roche, for lectures; and has served on Scientific Advisory Boards for DGM and Glykogenosis e.V. CGB reports study funding relating to the present manuscript paid to NINDS; and has participated in data safety monitoring or advisory boards without financial compensation, in his capacity of representing NIH. AMS is a principal investigator in the ASPIRO study. AB has received speaker's honoraria from Pfizer and Roche; and has participated in advisory boards at for Pfizer and Roche. SN, ARF, DNS, ET, and URQ report no conflicts of interests. MB and MJP are full-time employees of Diverge Translational Science Laboratory. EO and SD report no conflicts of interest. PK is a full-time employee of Diverge Translational Science Laboratory. SNK report no conflicts of interest. HM is a full-time employee of Diverge Translational Science Laboratory. MVA, CW, and HGD report no conflicts of interest. AHB received study funding relating to the present manuscript; reports grants or contracts received from NIH, MDA (USA), and the Chan Zuckerberg Initiative, and from AFM Telethon, Alexion Pharmaceuticals Inc., Avidity, Dynacure SAS, Kate Therapeutics, and Pfizer Inc. He has received consulting fees from Astellas Gene Therapies*, Dynacure, GLG Inc., Guidepoint Global, Kate Therapeutics, and Roche; has received support for attending meetings from Kate Therapeutics and MDA; holds equity in Kate Therapeutics and Kinea Bio, and is an inventor on a US patent describing a method for gene therapy of XLMTM. SC, EC, JL, CS, WM, BS (Sepulveda), FV are former employees of Astellas Gene Therapies*. ESJ and SR are former employees and stockholders in Astellas Gene Therapies*. SP was Chief Medical Officer and a stockholder in Astellas Gene Therapies* when the study was designed and initiated; he is no longer a stockholder and currently consults independently with a wide variety of companies and academic institutions primarily on Clinical Development matters.

*Formerly Audentes Therapeutics, Inc.

Acknowledgements

This study was funded by Astellas Gene Therapies, formerly Audentes Therapeutics, Inc.

We gratefully acknowledge the additional investigators involved in ASPIRO and in the INCEPTUS XLMTM Natural History Studies for their remarkable work in collecting part of the data: Laurent Servais, MD, Francesco Muntoni, MD, Barry Byrne, MD, PhD, Reshma Amin, MD, Carola Schön, MD, Francy Shu, MD, Katharina Vill, MD, and Ying Hu. We thank Caroline Finlay, MPH, Maria Candida Vila, PhD, PharmD, and Christina Chaivorapol, PhD, for operational and analytical support. We also acknowledge the valuable contributions of the independent Data Monitoring Committee: Gregory Enns, MB, ChB, Gerald Lipshutz, MD, David Rosenthal, MD, and Philip Rosenthal, MD. Medical writing support was provided by Joanne Fitz-Gerald, BPharm, of FourWave™ Medical Communications, funded by Astellas Gene Therapies, formerly Audentes Therapeutics, Inc.

Appendix A. Supplementary data

Supplementary data related to this article can be found at https://doi.org/10.1016/j.ebiom.2023.104894.

References

1 McEntagart M, Parsons G, Buj-Bello A, et al. Genotype-phenotype correlations in X-linked myotubular myopathy. *Neuromuscul Disord*. 2002;12(10):939–946.
2 Amburgey K, Tsuchiya E, de Chastonay S, et al. A natural history study of X-linked myotubular myopathy. *Neurology*. 2017;89(13):1355–1364.
3 Beggs AH, Byrne BJ, De Chastonay S, et al. A multicenter, retrospective medical record review of X-linked myotubular myopathy: the RECENSUS study. *Muscle Nerve*. 2018;57(4):550–560.
4 Annoussamy M, Lilien C, Gidaro T, et al. X-linked myotubular myopathy: a prospective international natural history study. *Neurology*. 2019;92(16):e1852–e1867.
5 Graham RJ, Muntoni F, Hughes I, et al. Mortality and respiratory support in X-linked myotubular myopathy: a RECENSUS retrospective analysis. *Arch Dis Child*. 2020;105(4):332–338.
6 Lawlor MW, Beggs AH, Buj-Bello A, et al. Skeletal muscle pathology in X-linked myotubular myopathy: review with cross-species comparisons. *J Neuropathol Exp Neurol*. 2016;75(2):102–110.
7 Buj-Bello A, Fougerousse F, Schwab Y, et al. AAV-mediated intramuscular delivery of myotubularin corrects the myotubular myopathy phenotype in targeted murine muscle and suggests a function in plasma membrane homeostasis. *Hum Mol Genet*. 2008;17(14):2132–2143.
8 Childers MK, Joubert R, Poulard K, et al. Gene therapy prolongs survival and restores function in murine and canine models of myotubular myopathy. *Sci Transl Med*. 2014;6(220):220ra10.
9 Elverman M, Goddard MA, Mack D, et al. Long-term effects of systemic gene therapy in a canine model of myotubular myopathy. *Muscle Nerve*. 2017;56(5):943–953.
10 Mack DL, Poulard K, Goddard MA, et al. Systemic AAV8-mediated gene therapy drives whole-body correction of myotubular myopathy in dogs. *Mol Ther*. 2017;25(4):839–854.
11 Shieh PB, Kuntz NL, Dowling JJ, et al. Safety and efficacy of gene replacement therapy for X-linked myotubular myopathy (ASPIRO): a multinational, open-label, dose-escalation trial. *Lancet Neurol*. 2023;22:1125–1139.
12 Lawlor MW, Shieh PB, Bönnemann CG, et al. LBP.13 ASPIRO gene replacement therapy trial with resamirigene bilparvovec in XLMTM: pathologic findings in three deceased study participants. [Poster presentation at the World Muscle Society (WMS) Virtual Congress 2021, September 20–24]. *Neuromuscul Disord*. 2021;31.
13 Mingozzi F, High KA. Immune responses to AAV vectors: overcoming barriers to successful gene therapy. *Blood*. 2013;122(1):23–36.
14 Nathwani AC, Tuddenham EG, Rangarajan S, et al. Adenovirus-associated virus vector-mediated gene transfer in hemophilia B. *N Engl J Med*. 2011;365(25):2357–2365.
15 Meng H, Janssen PM, Grange RW, et al. Tissue triage and freezing for models of skeletal muscle disease. *J Vis Exp*. 2014;89:51586.
16 Dubowitz V, Sewry C, Oldfors A. *Histological and histochemical changes. Muscle biopsy: a practical approach*. 5th ed. Elsevier; 2021:46–77.
17 Dastgir J, Rutkowski A, Alvarez R, et al. Common data elements for muscle biopsy reporting. *Arch Pathol Lab Med*. 2016;140(1):51–65.
18 Goddard MA, Mack DL, Czerniecki SM, et al. Muscle pathology, limb strength, walking gait, respiratory function and neurological impairment establish disease progression in the p.N155K canine model of X-linked myotubular myopathy. *Ann Transl Med*. 2015;3(18):262.
19 Gernoux G, Gruntman AM, Blackwood M, Zieger M, Flotte TR, Mueller C. Muscle-directed delivery of an AAV1 vector leads to capsid-specific T cell exhaustion in nonhuman primates and humans. *Mol Ther*. 2020;28(3):747–757.
20 Gernoux G, Guilbaud M, Devaux M, et al. AAV8 locoregional delivery induces long-term expression of an immunogenic transgene in macaques despite persisting local inflammation. *Mol Ther Methods Clin Dev*. 2021;20:20660–20674.
21 Lawlor MW, Read BP, Edelstein R, et al. Inhibition of activin receptor type IIB increases strength and lifespan in myotubularin-deficient mice. *Am J Pathol*. 2011;178(2):784–793.
22 Alfano LN, Dowling JJ, Shieh PB, et al. Improved muscle strength and attainment of motor milestones in boys with X-linked myotubular myopathy (XLMTM) administered single-dose gene replacement therapy (resamirigene bilparvovec, AT132). [Poster presented at the American Academy of Pediatrics (AAP) National Conference and Exhibition, 8–11 October 2021,Virtual]. *Pediatrics*. 2022;149(1 Meeting Abstracts February 2022):261.
23 Dowling JJ, Muller-Felber W, Smith BK, et al. INCEPTUS natural history, run-in study for gene replacement clinical trial in X-linked myotubular myopathy. *J Neuromuscul Dis*. 2022;9(4):503–516.
24 Molera C, Sarishvili T, Nascimento A, et al. Intrahepatic cholestasis is a clinically significant feature associated with natural history of X-linked myotubular myopathy (XLMTM): a case series and biopsy report. *J Neuromuscul Dis*. 2022;9(1):73–82.
25 Gangfuss A, Schmitt D, Roos A, et al. Diagnosing X-linked myotubular myopathy - a German 20-year follow up experience. *J Neuromuscul Dis*. 2021;8(1):79–90.
26 D'Amico A, Longo A, Fattori F, et al. Hepatobiliary disease in XLMTM: a common comorbidity with potential impact on treatment strategies. *Orphanet J Rare Dis*. 2021;16(1):425.